Decolorization of Rhodamine-B from Aqueous Solutions by Spent Mushroom Substrate

Jing Liu, Jinghao Shi, Chenxuan Qian, Yubo Zhao, Lihui Chen,* Liulian Huang, and Xiaolin Luo *

The adsorption of Rhodamine-B (Rh-B) from aqueous solutions onto spent mushroom substrate (SMS) and mushroom substrates prior to use (MSP) were comparatively studied in terms of the adsorption parameter effects, isotherms, and kinetics. It was found that an acidic pH of the dye solution was detrimental for basic Rh-B dye adsorption, which favored the electrostatic attraction between the cationic Rh-B and negative SMS and MSP. The adsorption isotherms of Rh-B onto the SMS and MSP followed the Langmuir model rather than the Freundlich or Temkin models. The fitted adsorption capacity of the SMS (107.5 mg/g) was approximately double that of the MSP (47.6 mg/g), which indicated a higher surface area and the presence of more adsorption functional sites that were created during edible fungus (*Grifola frondosa*) cultivation. Moreover, the experimental adsorption data of the SMS and MSP obeyed pseudo-second-order kinetics. The intraparticle diffusion plots revealed the multilinear adsorption nature of the SMS, which included boundary layer adsorption, intraparticle diffusion, and pore diffusion. However, only intraparticle diffusion played a major role in the adsorption of Rh-B onto MSP. It was concluded that the utilization of agricultural waste for edible fungus cultivation would not only improve the value of the agricultural waste itself, but can also remove Rh-B from aqueous solutions.

Keywords: Spent mushroom substrate (SMS); Mushroom substrates prior to use (MSP); Rhodamine-B (Rh-B); Adsorption; Isotherm; Kinetics

*Contact information: College of Materials Engineering, Fujian Agriculture and Forestry University, Fuzhou 350002, China; *Corresponding authors: xluo53@163.com; lihuichen66@126.com*

INTRODUCTION

Nowadays, to improve application performances, many dyes are synthesized with improved properties, such as thermal stability, photo-resistance, and chemical resistance (Qu *et al*. 2015). These virtues allow these dyes to meet various commercial demands and increased competition. However, large volumes of wastewater are produced during the textile printing and dyeing processes (Gao *et al*. 2016). Some dyes contained in wastewater not only deteriorate the water quality, but they also cause a noticeable impact on humans and aquatic organisms. For instance, Rhodamine B (Rh-B), a basic red dye in the xanthenes class that is widely used in the paint, textiles, paper, and leather industries, has been experimentally shown to be carcinogenic and mutagenic to the marine food chain (Tan *et al.* 2014). Therefore, removing Rh-B from aqueous effluents has attracted much attention worldwide.

To date, various methods have been developed for removing Rh-B from contaminated water, including chemical oxidation (Nadupalli *et al*. 2011), photodegradation (Zhang *et al*. 2016b), biodegradation (Shenvi *et al*. 2015), adsorption

onto inorganic (Zhang *et al.* 2012; Tehrani and Zare-Dorabei 2016) or organic materials (Gupta *et al.* 2000; Zhang *et al.* 2016a), and more. Since Rh-B is not only stable under heat and light, but also resistant to oxidation and biodegradation, adsorption is considered to be the most effective method for removal (Gao *et al.* 2015). Of the adsorption technologies, inorganic and inorganic-organic hybrid materials, such as activated carbon (Guo *et al.* 2005; Ding *et al.* 2014), zeolites (Wang *et al.* 2006; Hu *et al*. 2015), and metal-organic frameworks (Liu *et al.* 2016; Tehrani and Zare-Dorabei 2016), have been investigated thoroughly. Though these materials have been shown to be efficient at removing Rh-B from wastewater, both their application and scale-up are limited because of the high costs and complex synthesis processes. Thus, it is of great importance to discover materials that are natural, organic, and inexpensive for the efficient removal of Rh-B.

Low-cost natural materials used to remove Rh-B mainly come from agricultural by-products, such as bagasse fly ash (Gupta *et al.* 2000), mango leaf powder (Khan *et al.* 2011), fruit epicarp (Inyinbor *et al*. 2016), sawdust (Abdulsalam and Oladipo 2015), jute stick powder (Panda *et al.* 2009), and more. It is well known that sawdust and other agricultural by-products are necessary raw materials for edible mushroom production (Obodai *et al.* 2003). These agricultural by-products can also be re-utilized with corresponding solid resides, which results in adsorption abilities that are as good as or better than those of the original by-products (Tian *et al.* 2011; Toptas *et al.* 2014). Recently, the use of spent mushroom substrate (SMS), a waste product from the process of mushroom production, as an adsorbent for removing different kinds of dyes from wastewater has been investigated. Tian *et al.* (2011) investigated the use of SMS in decolorizing textile effluent and achieved a maximum adsorption capacity of approximately 148 mg/g for Congo Red. Additionally, Yan and Wang (2013) used SMS to remove Methylene Blue from aqueous solutions and reached a maximum adsorption capacity of approximately 64 mg/g. Afterwards, SMS was also used to treat wastewater contaminated with Acid Red 111 or Basic Red 18 (Toptas *et al.* 2014). However, to the best of the knowledge of the authors, research on the use of SMS to remove Rh-B from dye effluents has not been conducted. To expand the application field of SMS, it is imperative to conduct comparative studies on the adsorption behavior of SMS and mushroom substrates prior to use (MSP).

In addition to using SMS to treat wastewater, its regeneration or re-utilization is also important. Typically, contaminated SMS was recovered by solution-washing. For example, acid (HNO_3) and alkali (NaOH) solution with different concentration were applied to regenerate *Azolla pinnata* adsorbed by Rh-B (Kooh *et al.* 2016). For desorption of Rh-B from inorganic adsorbents (metal-organic framework (MOF) and carbon nanotube, etc.), some salt solutions including $CaCl_2$ and NaCl, and solvent such as acetone had been found to be effective (Huo and Yan 2012; Liu *et al.* 2016). Although the performance of these solutions on the desorption of Rh-B from SMS or MSP is limited, it deviates from the focus of this study.

Thus, the purpose of this study was to evaluate the potential of SMS as a low-cost alternative adsorbent for removing Rh-B from wastewater. The effects of the initial dye concentration, initial solution pH, and contact time on the adsorption properties of SMS and MSP were compared. Corresponding isotherms and kinetics of the adsorption processes were also analyzed.

EXPERIMENTAL

Materials

SMS and MSP were generously provided by the Mycological Research Center of Fujian Agriculture and Forestry University, China. MSP contains 22 wt.% corn stalk powder, 50 wt.% cotton seed hull, 26 wt.% wheat bran, and 2 wt.% lime. Prior to use, corn stalk, cotton seed hull, and wheat bran were ground in a Wiley mill, screened to pass through a 40-mesh screen, and then sealed in plastic bags until further use. *Grifola frondosa* was cultivated on MSP. After manually removing the edible fungus and washing it with deionized (DI) water, SMS was obtained, which is a waste from *Grifola frondosa* cultivation.

Rh-B (CAS Reference Number: 81-88-9, Molecular Formula: $C_{28}H_{31}ClN_2O_3$, Molecular Weight: 479.01, maximum ultraviolet adsorption wavelength (λ_{max}): 554 nm) was purchased from Sigma-Aldrich (Shanghai, China) and used without further purification. Rh-B is a basic red dye that is water soluble and part of the xanthenes class. It is suggested to not come in direct contact with Rh-B because of its high toxicity, quick coloration of human skin, and irritation of skin and eyes. The chemical structure of Rh-B is shown in Fig. 1.

Batch Adsorption

The adsorbents, SMS and MSP, were both washed with DI water until they had a neutral pH. Clean SMS and MSP were then air dried 3 d before use. Batch adsorption was performed in 250-mL sealed triangle flasks with 100 mL of dye solution that had a concentration ranging from 20 to 1000 mg/L. The flasks were shaken on an incubator (MaxQ 481 HP, Thermo Fisher Scientific, Waltham, USA) at 25 °C with a stirring speed ranging from 90 to 180 rpm. The initial pH of the dye solution was adjusted using 0.1 mol/L HCl or NaOH. The influences of the adsorbent dosage (0.1 to 1.5 g) and stirring speed (90 to 180 rpm) were also evaluated in the present study.

For the isothermal adsorption experiments, adsorption was sustained for 1 h, which was sufficient to reach equilibrium. The base solution of Rh-B was prepared with DI water and diluted as required. For the adsorption kinetic experiments, adsorption was carried out with the following conditions: 1 g of SMS, 100 mL of dye solution (20, 50, and 100 mg/L), stirring speed of 150 rpm, and 25 °C. The sampling time ranged from 1 to 60 min. After sampling the dye solution, it was centrifuged for the dye concentration measurement.

Dye Concentration Measurement

All of the sampled filtrates were first centrifuged at 10,000 rpm for 5 min. The supernatants were analyzed for the residual Rh-B concentration with an ultraviolet visible (UV-Vis) spectrophotometer (Agilent 8453, USA) at the maximum wavelength (λ_{max}) of 554 nm. DI water was used as the background sample for the UV-Vis measurement. A standard curve was developed using a set of Rh-B solutions with a concentration gradient. The adsorption capacity at the equilibrium time (q_e, mg/g), amount of dye adsorbed at the measured time (q_t, mg/g), and dye removal (DR, %) of the SMS and MSP were calculated according to the following equations,

$$q_e = \frac{(C_0 - C_e) \times v}{m} \quad (1)$$

$$q_t = \frac{(C_0 - C_t) \times v}{m} \quad (2)$$

$$DR = \frac{(C_0 - C_e) \times 100}{C_0} \quad (3)$$

where C_0 is the initial dye concentration (mg/L), C_e is the residual dye concentration at equilibrium (mg/L), m is the mass of the adsorbent (g), v is the volume of the adsorption solution (L), and C_t is the dye concentration at time t (mg/L).

RESULTS AND DISCUSSION

Effects of the Initial Solution pH, Adsorbent Dosage, and Stirring Speed on the Equilibrium Adsorption Capacity and Removal of Rh-B

Because of changes in the adsorbent surface charge and ionization degree of the dye molecule, the initial pH value of the dye solution is regarded as one of the most important factors affecting adsorption. Figure 2a shows the effect of the dye solution pH on the adsorption capacities of Rh-B onto the SMS and MSP. It was obvious that the equilibrium adsorption capacities (q_es) of Rh-B onto the SMS and MSP decreased from 2.0 to 1.5 mg/g and 1.4 to 1.2 mg/g, respectively, as the pH value of the initial solution increased from 2 to 4, and then gradually reached a constant value as the pH became near neutral and basic. This result could have been caused by the surface charge of the adsorbent or ionization forms of the Rh-B at different pH values. Toptas *et al.* (2014) reported that the surface charge of washed SMS exhibited an increasing negativity as the pH of the dye solution was increased from 2 to 11. The ζ-potential of the SMS ranged from -1 to -4 mV and -4 to -14 mV when the pH of the dye solution ranged from 1 to 3 and 3 to 11, respectively (Fig. 1). Biomass, including corn stalk powder, cotton seed hull, and wheat bran, is composed mainly of lignin, cellulose, hemicellulose, and extractives (Luo *et al.* 2014). Because of the –OH functional group from phenols, alcohols, and carboxylic acids in the lignin and carbohydrates, the surface charge of the washed MSP is believed to be negative (Chen *et al.* 2004). At a pH less than 3, the Rh-B molecules existed in a monomeric cation form, and a strong electrostatic attraction between the cationic Rh-B and negative SMS and MSP was favored. At a pH greater than 3, the Rh-B molecules were in zwitterionic form in solution (Fig. 1), which could have caused them to aggregate into bigger molecules. This decreased the positive charge density of the Rh-B, which then led to the gradual disappearance of electrostatic interaction between the Rh-B and negative SMS and MSP. As the number of H^+ ions released from the carboxylic groups increased and Rh-B molecules continued to aggregate, the repulsion force between the adsorbate and adsorbent may have increased accordingly. Additionally, the small pore sizes of SMS and MSP were not easily accessible for the bigger Rh-B molecules. These findings were similar to the results of cationic sulfa antibiotics adsorption onto SMS (Zhou *et al.* 2016). Although the adsorption capacity of the SMS and MSP both decreased as the pH of the Rh-B solution increased from 2 to 11, the q_e of the former was remarkably higher than that of the latter because of larger pore sizes and pore volumes formed during the process of edible fungus cultivation (Toptas *et al.* 2014). According to the above discussion, lower pH values of the Rh-B solution, such as 2, is more favorable for increasing the adsorption capacity of the

SMS and MSP. Therefore, the relatively optimum initial pH value of the Rh-B solution was determined to be 2. The following experiments were all conducted at this pH.

The effects of the adsorbent dosage on Rh-B removal and the equilibrium adsorption capacities (q_es) are shown in Fig. 2b. Rh-B removal initially increased with the increase in the SMS and MSP dosages, and then it was a constant value. For example, with a dye solution volume of 100 mL, the Rh-B removal increased from 60.4% to a constant value of 99.3% when the SMS dosage was increased from 0.1 to 1.2 g. The Rh-B removal increased from 19.7% to a constant value of 85.0% with MSP at the same dosages, which was far lower than that of SMS. This may been because of the higher number of available adsorption functional sites and greater adsorbent surface area created by the edible fungus (Tian *et al.* 2011; Toptas *et al.* 2014). However, the q_e decreased gradually with increasing dosages of SMS and MSP, which showed that the adsorption saturation capacity of Rh-B onto the SMS and MSP had not been reached with a dye concentration of 20 mg/L. A greater adsorbent surface area and more adsorption functional sites were available to treat the dye waste solution with a high concentration. Thus, a higher Rh-B concentration was used to evaluate the adsorption isotherms in the following sections.

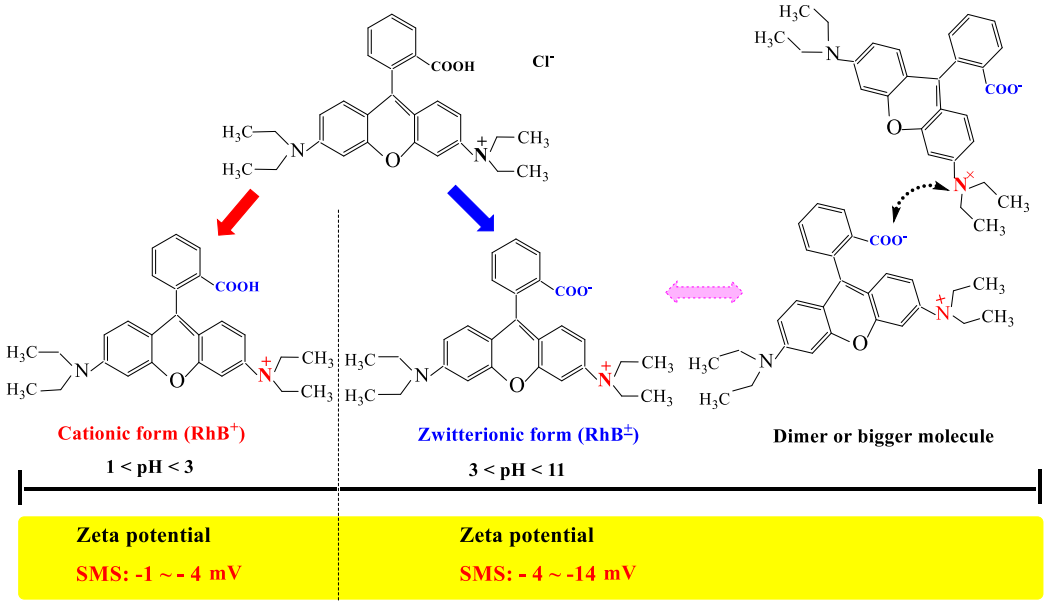

Fig. 1. Effect of the solution pH on the ζ-potential and molecular form of the Rh-B

According to the reference (Wu *et al.* 2017), the permissibly detectable concentration of RhB is 500 μg/kg, which was already established by Europe and USA. With the highest Rh-B removal (99.3%) achieved by SMS, the concentration of Rh-B (0.14 mg/kg) left in wastewater does not exceed above limit, suggesting that no extra treatments are required to reach a safe concentration level of Rh-B.

The effect of the stirring speed on the q_es of the Rh-B onto the SMS and MSP was also investigated (Fig. 2c). It was found that for MSP, the q_e increased slightly when the stirring speed increased from 90 to 180 rpm. However, for SMS, the q_e of the Rh-B did not change remarkably with an increase in the stirring speed. This meant that the adsorption balance could easily be reached at a lower stirring speed because there were enough adsorption functional sites and surface area on the SMS for Rh-B to adhere. To avoid the stirring speed effect on the following adsorption isotherms and kinetics analyses, the stirring speed was set at 150 rpm.

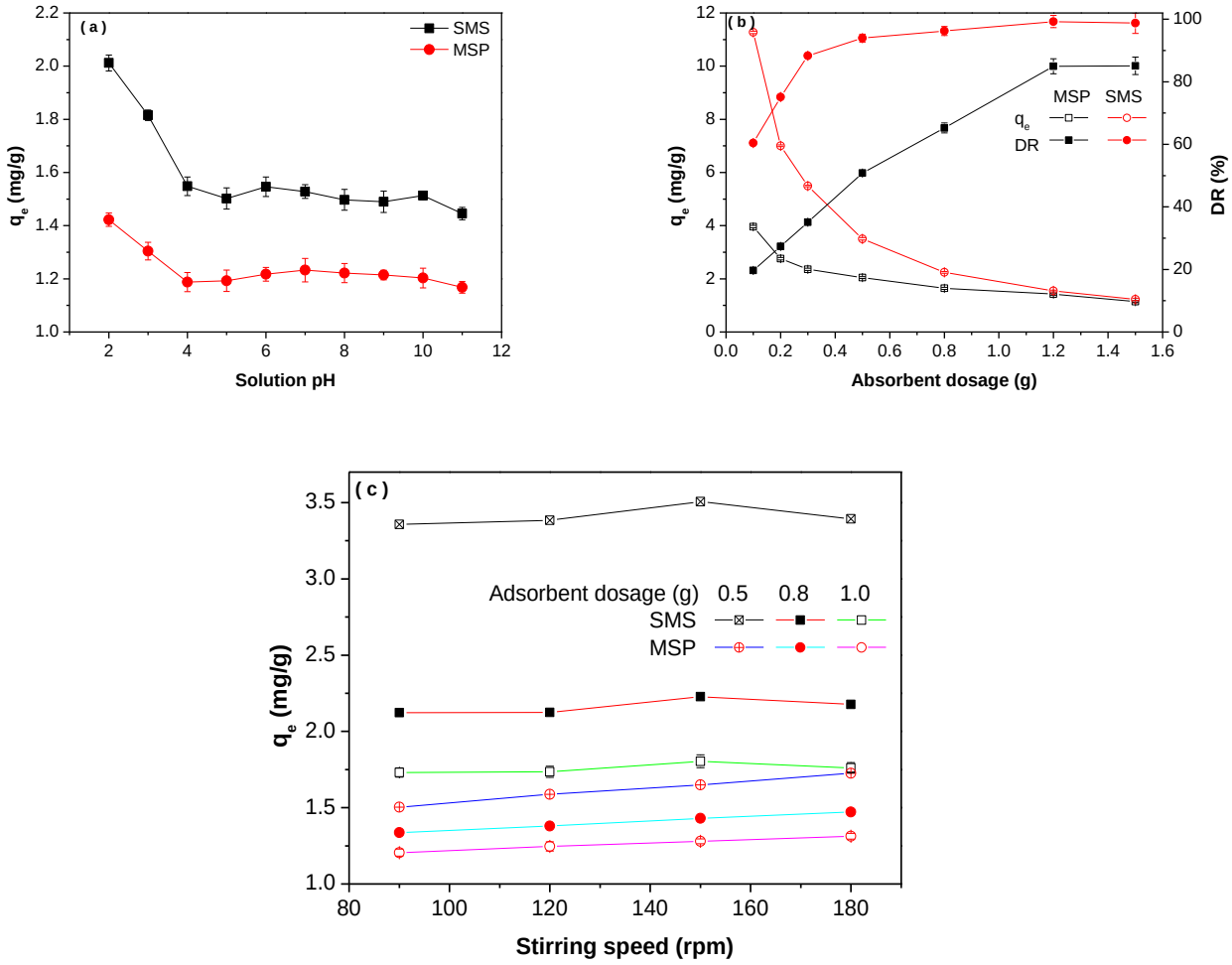

Fig. 2. Effects of the pH (a), adsorbent dosage (b), and stirring speed (c) on the equilibrium adsorption capacity and removal of Rh-B with SMS and MSP. The temperature, Rh-B concentration and the volume of Rh-B solution for all adsorptions were set as 298 K, 20 mg/L and 100 mL, respectively. For investigating the pH of Rh-B solution (Fig. 2. (a)), adsorbent dosage and stirring speed were fixed as 1 g and 150 rpm; for investigating adsorbent dosage (Fig. 2. (b)), the pH of Rh-B solution and stirring speed were fixed as 2 and 150 rpm; for investigating stirring speed (Fig. 2. (c)), the pH of Rh-B solution was 2. The standard deviations of duplicates were expressed via error bars on all figures.

Adsorption Isotherms of Rh-B onto the SMS and MSP

Adsorption isotherm models, including the Langmuir, Freundlich, and Temkin models, are usually used to explain the equilibrium relationship between an adsorbent and adsorbate (Ruthven 1984). The Langmuir isotherm model is often applied for homogeneous monolayer adsorption onto a surface with a finite number of identical sites. Its known expression and derived linear form are expressed as follows,

$$\frac{q_e}{q_m} = \frac{K_L C_e}{1 + K_L C_e} \quad (4)$$

$$\frac{1}{q_e} = \frac{1}{q_m} + \frac{1}{K_L q_m} * \frac{1}{C_e} \quad (5)$$

where q_m is the maximum theoretical adsorption capacity (mg/L) and K_L represents the Langmuir constant related to the energy of adsorption (L/mg).

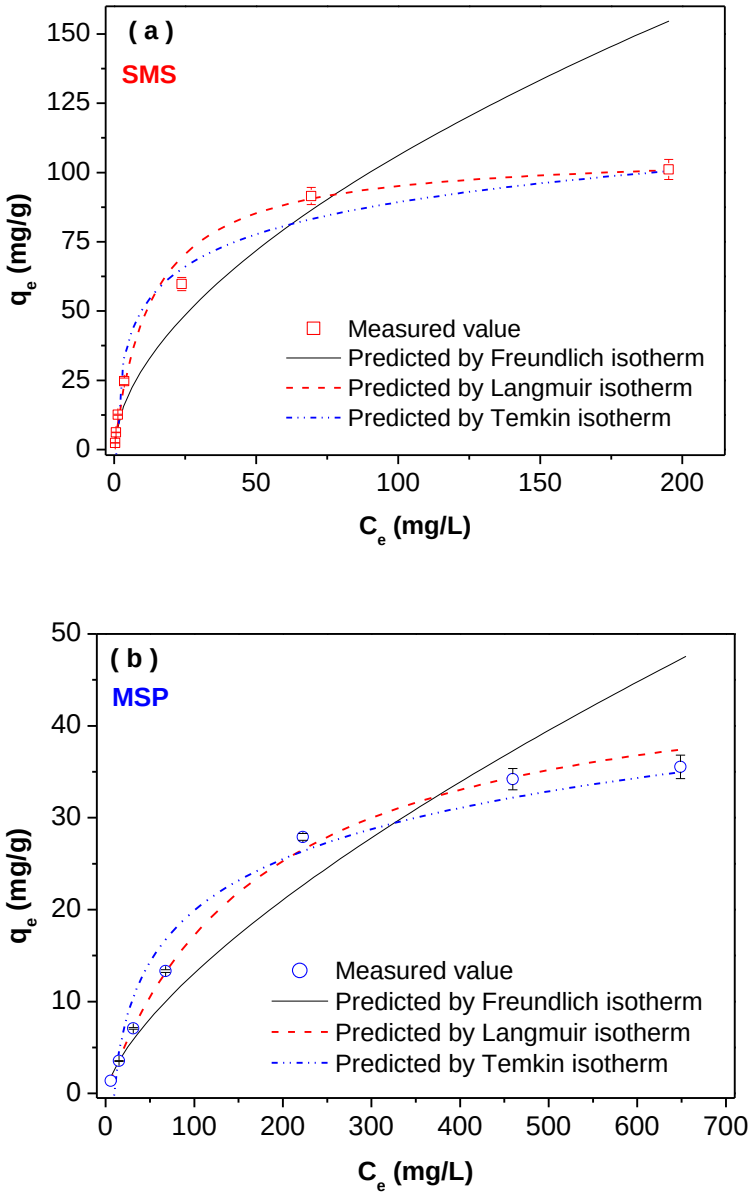

Fig. 3. Adsorption isotherms of Rh-B onto the SMS (a) and MSP (b) with an adsorbent dosage, dye solution pH and volume, stirring speed, and solution temperature of 0.8 g, 2 and 100 mL, 150 rpm, and 25 °C, respectively. The error bars on graphs are standard deviations of duplicates.

The Freundlich isotherm model and its linear expression, which are widely used to describe non-ideal adsorption onto heterogeneous surfaces with different functional sites and different kinds of adsorbent-adsorbate interactions, is shown below,

$$q_e = K_F (C_e)^{1/n} \quad (6)$$

$$\ln q_e = \ln K_F + \frac{1}{n} \ln(C_e) \quad (7)$$

where K_F ((mg/g)·(L/mg)$^{1/n}$) is the adsorption capacity of the adsorbent and n is the intensity of adsorption.

The Temkin isotherm model describes chemical adsorption involving the heat of adsorption and adsorbent-adsorbate interaction. The original and derived linear formulas are expressed as follows,

$$q_e = \frac{RT}{\Delta Q} \ln K_0 C_e \quad (8)$$

$$q_e = \frac{RT}{\Delta Q} * \ln K_0 + \frac{RT}{\Delta Q} * \ln C_e \quad (9)$$

where R is the universal gas constant (J/(mol·K)), T is the solution temperature (K), ΔQ is the variation in the adsorption energy (J/mol), and K_0 is the equilibrium binding constant (L/mg).

For adsorption of Rh-B onto the SMS and MSP, it was observed that higher coefficients of determination ($R^2 > 0.99$) were achieved with the Langmuir isotherm model (Table 1), which indicated a better fit with this model compared with the other two isotherm models. This result was similar to the results of Congo Red adsorption onto SMS, whose experimental data was better fit by the Langmuir isotherm model than the Freundlich and Temkin isotherm models (Tian *et al.* 2011). Therefore, the assumption was made that the coverage of Rh-B onto the adsorptive sites of the SMS and MSP was a monolayer.

Table 1. Isotherm Adsorption Parameters of Rh-B onto the SMS and MSP

	SMS	MSP
Freundlich isotherm		
K_F	7.945	0.553
n	1.777	1.456
R^2	0.929	0.964
Langmuir isotherm		
q_m	107.527	47.619
K_L	0.077	0.006
R^2	0.998	0.995
Temkin isotherm		
ΔQ	15.913	14.660
K_0	2.072	0.119
R^2	0.975	0.960

As shown in Fig. 3, the adsorption capacity of the SMS and MSP was enhanced with the increase in the initial Rh-B concentration. However, it was also seen from Table 1 that the maximum monolayer adsorption capacity of the SMS for Rh-B was approximately double that of the MSP. This was attributed to the higher surface area and more adsorption functional sites, which mainly come from the biological digestion reaction of *Grifola frondosa* on lignocellulose (corn stalk powder, cotton seed hull, and wheat bran) during the process of cultivation. Moreover, Al-Degs *et al.* (2008) stated that a higher value of K_L in the Langmuir isotherm model was indicative of a favorable adsorption process. By comparing the two K_L values, it was concluded that the adsorption of Rh-B onto SMS

was more favorable than onto MSP. This was consistent with the fitting results from the other two models, although the fitting degree of each of those models was not as good as that of the Langmuir isotherm model (Table 1).

In addition to the Langmuir K_L constant, the favorable nature of adsorption can be expressed with the dimensionless separation factor (R_L), which is an important indicator of the adsorption process and is calculated by the following equation,

$$R_L = \frac{1}{1 + K_L C_0} \quad (10)$$

where K_L is the Langmuir constant related to the energy of adsorption (L/mg) and C_0 is the initial dye concentration (mg/L). The value of R_L indicates whether the adsorption process is irreversible ($R_L = 0$), favorable ($0 < R_L < 1$), linear ($R_L = 1$), or unfavorable ($R_L > 1$).

For the separation factors of Rh-B adsorption onto the SMS and MSP, Fig. 4 showed that the values of R_L were all within the range of 0 to 1, which confirmed that SMS and MSP were both favorable for the adsorption of Rh-B under the investigated conditions.

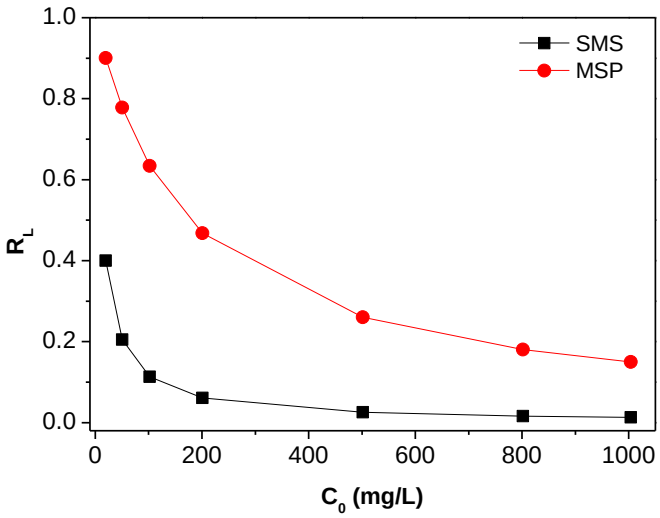

Fig. 4. Separation factors of Rh-B adsorption onto the SMS and MSP with an adsorbent dosage, dye solution pH and volume, stirring speed, and solution temperature of 0.8 g, 2 and 100 mL, 150 rpm, and 25 °C, respectively

Adsorption Kinetics of Rh-B onto the SMS and MSP

As shown in Figs. 5a and 5b, the variations in the adsorption capacities at the dye concentrations of 20, 50, and 100 mg/L underwent three distinct stages. The time-dependent adsorption capacities of the MSP and SMS rapidly increased in the initial 15 min, then slowed down, and finally reached equilibrium. According to the research by Zhang *et al.* (2016a), the first adsorption stage was a general physi-diffusion or physi-sorption, which was attributed to the rough and irregular surface of the adsorbent. Chemi-sorption, such as ion-exchange between active functional sites with Rh-B, mainly occurred in the second stage. Therefore, the rate-limiting step of biosorption could be determined.

Additionally, the adsorption capacities also increased with the initial dye concentration, which indicated that adsorption was favorable at high concentration of Rh-B. For the three dye concentrations, the adsorption capacities of the SMS were all noticeably higher than that of the MSP (Figs. 5a and 5b), which was consistent with the

results from Figs. 2b and 3. This was mainly caused by a higher surface area and more active functional sites on the SMS than the MSP. Thus, these three dye concentrations were selected to investigate the kinetic adsorption behaviors of Rh-B onto the SMS and MSP. To determine the exact adsorption rate of Rh-B onto the MSP and SMS, kinetic models were developed and analyzed, and are shown in Fig. 5.

Rh-B adsorption usually follows a pseudo-second-order kinetic model (Abdulsalam and Oladipo 2015; Liu *et al.* 2016; Zhang *et al.* 2016a). To investigate the adsorption process, two kinds of kinetic models, pseudo-first-order and pseudo-second-order, were used to fit the experimental data. The pseudo-first-order kinetic equation is shown in Eq. 11:

$$\frac{dq_t}{dt} = k_1(q_e - q_t) \tag{11}$$

Integrating Eq. 11 with the initial conditions ($q_t = 0$ at $t = 0$ min and $q_t = q_t$ at $t = t$ min) resulted in the derived form shown as the following equation:

$$\ln(q_e - q_t) = \ln q_e - k_1 t \tag{12}$$

where k_1 is the rate constant of the equation (min^{-1}).

If the adsorption of Rh-B follows the pseudo-first-order kinetic equation, there should be a linear relationship between $\ln(q_e - q_t)$ and t. From Figs. 5c and 5d, it was found that a linear curve was only achieved by MSP and not by SMS. The value of k_1 and q_e were calculated from the slope and intercept of the linear line on the graph. However, the calculated equilibrium adsorption capacities (q_es) were all lower than the corresponding experimental q_es, which indicated that the experimental data of Rh-B adsorption onto the MSP was not fitted well by the pseudo-first-order equation. For pseudo-first-order kinetic equation, a non-goodness-of-fit for Rh-B and other basic dyes onto bio-adsorbents and inorganic adsorbents was reported by previous researchers as well (Wang *et al.* 2006; Tian *et al*. 2011; Toptas *et al.* 2014; Qu *et al.* 2015; Gao *et al.* 2016; Zhang *et al.* 2016a).

In order to further investigate the kinetic adsorption of Rh-B onto the MSP and SMS, the pseudo-second-order equation was applied. It was expressed as:

$$\frac{dq_t}{dt} = k_2(q_e - q_t)^2 \tag{13}$$

By taking into account the boundary conditions ($q_t = 0$ at $t = 0$ min and $q_t = q_t$ at $t = t$ min) and rearranging Eq. 13, Eq. 14 was derived:

$$\frac{t}{q_t} = \frac{1}{k_2 q_e^2} + \frac{t}{q_e} \tag{14}$$

where k_2 is the rate constant for the pseudo-second-order adsorption equation (g/(mg·min)).

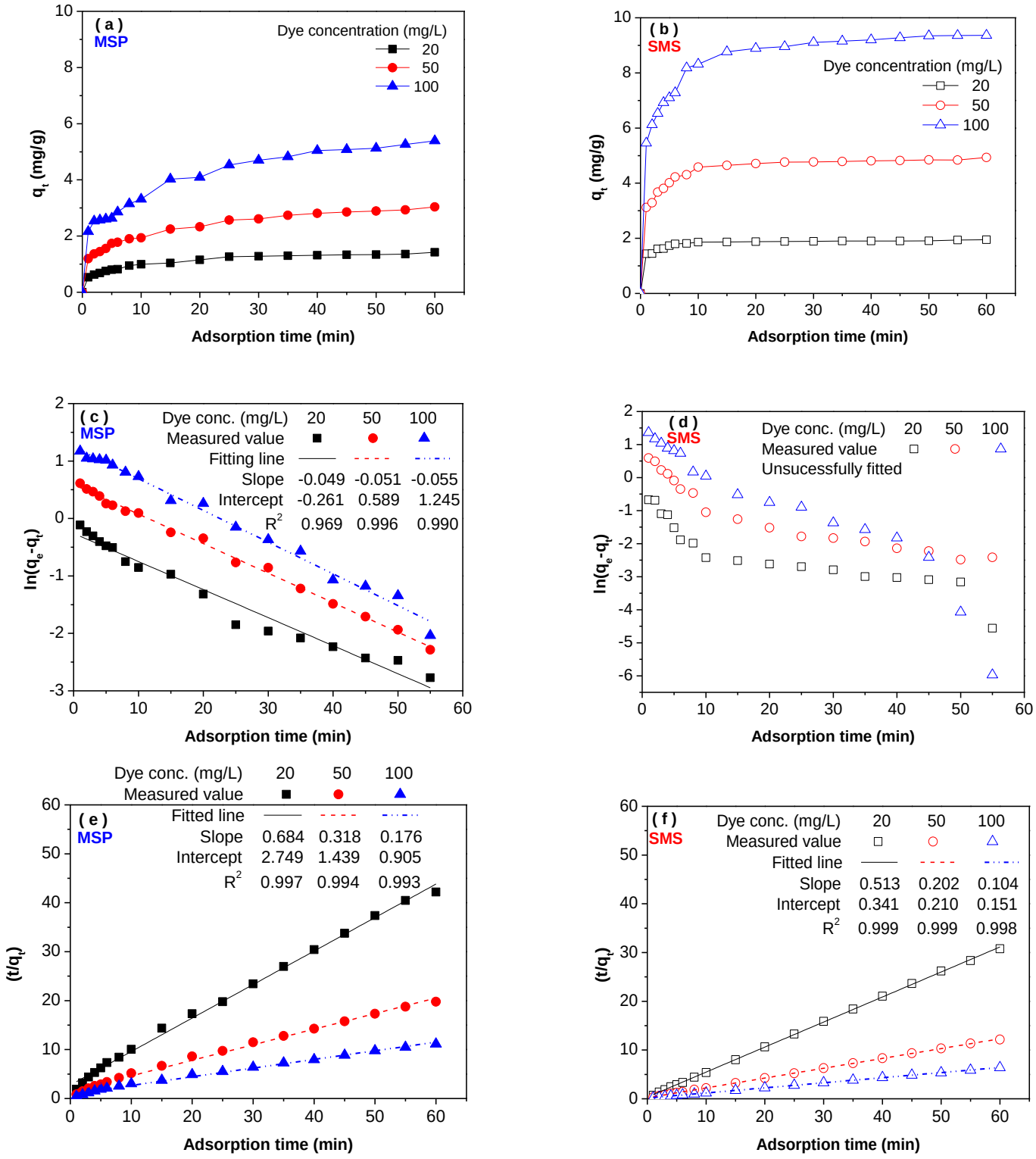

Fig. 5. Adsorption kinetics of Rh-B onto the MSP (a, c, and e) and SMS (b, d, and f) with an adsorbent dosage, dye solution pH and volume, stirring speed, and solution temperature of 1.0 g, 2 and 100 mL, 150 rpm, and 25 °C, respectively

Table 2. Kinetic Parameters of Rh-B Adsorption onto the SMS and MSP

Adsorbent	C_0 (mg/L)	Experimental q_e (mg/g)	Pseudo-First-Order			Pseudo-Second-Order		
			Calculated q_e (mg/g)	k_1	R^2	Calculated q_e (mg/g)	k_2	R^2
	20	1.42	0.79	0.049	0.971	1.46	0.163	0.997
	50	3.03	1.80	0.051	0.997	3.14	0.070	0.995
	100	5.39	3.47	0.055	0.990	5.66	0.035	0.994
	20	1.94	-	-	-	1.95	0.773	0.971
	50	4.93	-	-	-	4.96	0.194	0.999
	100	9.36	-	-	-	9.57	0.072	0.999

As shown in Figs. 5e and 5f, the time-dependent adsorption of Rh-B onto the MSP and SMS were well described by the pseudo-second-order equation. The plots of e/q_t against t had straight lines. Table 2 lists the results of q_e, k_2, and R^2 for the three initial concentrations of Rh-B on the MSP and SMS. For the dye solutions concentration of 20 and 100 mg/L, the coefficient of determination (R^2) for Rh-B adsorption onto the MSP from the pseudo-second-order kinetics was slightly higher than that from the pseudo-first-order kinetics by about 3 and 0.3%. However, the R^2 values for the three initial concentrations of Rh-B on the SMS were all above 0.99, which suggested that the second-order biosorption was the best fit for the adsorption process. Similar results were reported by Gupta *et al.* (2000), Tian *et al.* (2011), Yan and Wang (2013), and Zhang *et al.* (2016a).

The values of q_e and k_2 were determined from the slopes and intercepts of the plots (Figs. 5e and 5f). The equilibrium adsorption capacity (q_e) of the SMS increased from 1.95 to 9.57 mg/g as the initial dye concentration increased from 20 to 100 mg/L, which was noticeably higher than that of the MSP. Moreover, the k_2 of SMS and MSP both decreased as the initial dye concentration increased, but the k_2 of the former was higher than that of the latter at all of the dye concentration levels. The higher values of q_e and k_2 for the SMS were mainly caused by more negative functional sites. This was because after edible fungus (*Grifola frondosa*) cultivation, more Lewis base sites were created in the SMS than in the MSP (Yan and Wang 2013; Zhou *et al.* 2016). Thus, it was concluded that the utilization of agricultural waste for edible fungus cultivation not only improves the value of the agricultural waste itself, but can also treat dye wastewater.

Intraparticle Diffusion of Rh-B during Adsorption by SMS and MSP

The adsorbate is mainly transported from the bulk solution into the solid phase of adsorbent through an intraparticle diffusion process. To further elucidate the adsorption mechanism of the Rh-B onto the SMS and MSP, an empirical model called the Weber-Morris plot was used, and is shown below:

$$q_t = k_i \sqrt{t} + C \tag{15}$$

where k_i is the intraparticle diffusion rate constant (mg/(g·min$^{1/2}$)) and C is the intercept of the plot.

With Eq. 15, Ruthven (1984) and Khan *et al.* (2011) pointed out that a plot of q_t *versus* $t^{1/2}$ should be a straight line that goes through the origin of the intraparticle diffusion, which indicates it is the sole rate-limiting step. The intraparticle diffusion plots for the MSP and SMS are given in Figs. 6a and 6b. Although the plots of q_t *versus* $t^{1/2}$ for the adsorption of Rh-B onto the MSP were linear, they did not pass through the origin. This indicated that

even though intraparticle diffusion played a major role in the adsorption of Rh-B onto the MSP, it was not the sole rate-limiting step. From Fig. 6b, it was found that the adsorption process was multilinear. This suggested that more than one factor affected the adsorption of Rh-B onto the SMS, such as surface sorption and intraparticle diffusion (Inyinbor *et al.* 2016). Moreover, the intercept of the first linear portion of the plot was not zero. This implied that the initial stage of the plot involved boundary layer adsorption, while the second linear portion was because of intraparticle or pore diffusion (Yan and Wang 2013). Because different adsorption pathways were used to remove dye from the waste solution, it was determined that the multilinear nature of Rh-B adsorption onto the outer and inner surface areas of the SMS was an important part of adsorption.

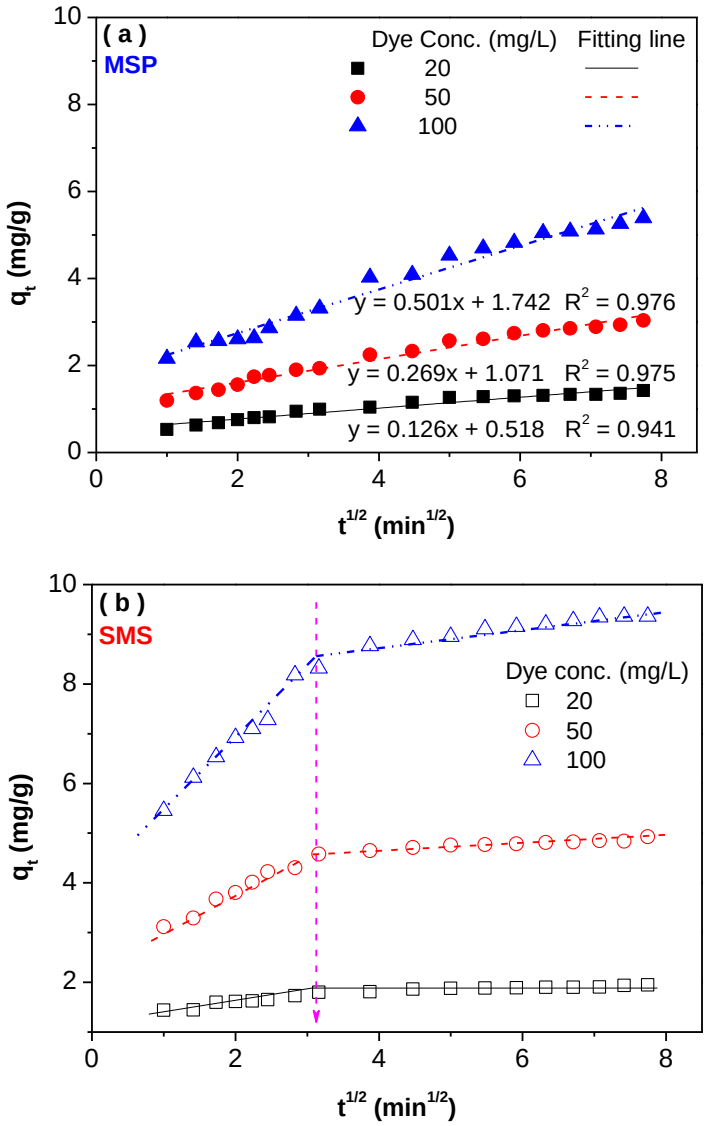

Fig. 6. Intraparticle diffusion plots for Rh-B adsorption onto the MSP (a) and SMS (b) with an adsorbent dosage, dye solution pH and volume, stirring speed, and solution temperature of 1.0 g, 2 and 100 mL, 150 rpm, and 25 °C, respectively

These findings were in agreement with the results from the isotherms and kinetics analyses performed. Edible fungus cultivation resulted in more pores and active functional

sites on the inner surface of the SMS, which determined the multilinear nature of the adsorption process. The research by Luo and Zhu (2011) demonstrated that the inner surface area of chemically or biologically treated lignocellulose was normally 100 times larger than the external surface area. Therefore, SMS possessed a superior adsorption capacity when compared with MSP.

CONCLUSIONS

1. An acidic pH of the initial dye solution, such as 2, resulted in the cationic form of Rhodamine-B (Rh-B), which promoted the electrostatic attraction between the cationic Rh-B and negative spent mushroom substrate (SMS) and mushroom substrate prior to use (MSP). For Rh-B concentrations ranging from about 20 to 1000 mg/L, the processing conditions of SMS involving adsorbent dosage, dye solution pH, stirring speed, and solution temperature were optimized as 0.8~1 g, 2, 150 rpm, and 25 °C, respectively, resulting in a dye removal (DR) that decreased from about 99 to 80%.
2. The fitted Langmuir model revealed that SMS had a higher adsorption capacity than MSP.
3. The results from the pseudo-second-order kinetics and intraparticle diffusion plots indicated that edible fungus (*Grifola frondosa*) cultivation resulted in a higher surface area and more adsorption functional sites in the SMS than MSP. It was shown that SMS had a multilinear adsorption behavior, indicating that more than one mechanism was involved in the removal of Rh-B from aqueous solutions.

ACKNOWLEDGMENTS

The funding from Fujian Provincial Department of Education (No. JB13033, JA15181, JA14098, and New Century Excellent Talents Supporting Plan (Min [2015]54)), Postdoctoral Science Foundation of China (2015M571955) and Department of Forestry (No.6, Min Forestry 2013) are gratefully acknowledged.

REFERENCES CITED

Abdulsalam, K., and Oladipo, M. A. (2015). "Adsorption of rhodamine B from single, binary and ternary dye systems using sawdust of *Parkia biglobosa* as adsorbent: Isotherm, kinetics and thermodynamics studies," *J. Chem. Pharm. Res.* 7(2), 454-475.

Al-Degs, Y. S., El-Barghouthi, M. I., El-Sheikh, A. H., and Walker, G. M. (2008). "Effect of solution pH, ionic strength, and temperature on adsorption behavior of reactive dyes on activated carbon," *Dyes Pigments* 77(1), 16-23. DOI: 10.1016/j.dyepig.2007.03.001

Chen, S.-L., Wang, S., and Lucia, L. A. (2004). "New insights into the fundamental nature of lignocellulosic fiber surface charge," *J. Colloid Interf. Sci.* 275(2), 392-397. DOI: 10.1016/j.jcis.2004.02.010

Ding, L., Zou, B., Gao, W., Liu, Q., Wang, Z., Guo, Y., Wang, X., and Liu, Y. (2014). "Adsorption of Rhodamine-B from aqueous solution using treated rice husk-based activated carbon," *Colloid. Surface. A* 446, 1-7. DOI: 10.1016/j.colsurfa.2014.01.030

Gao, Y., Wang, Y., and Zhang, H. (2015). "Removal of Rhodamine B with Fe-supported bentonite as heterogeneous photo-Fenton catalyst under visible irradiation," *Appl. Catal. B-Environ.* 178, 29-36. DOI: 10.1016/j.apcatb.2014.11.005

Gao, Y., Xu, S., Yue, Q., Wu, Y., and Gao, B. (2016). "Chemical preparation of crab shell-based activated carbon with superior adsorption performance for dye removal from wastewater," *J. Taiwan Inst. Chem. E.* 61, 327-335. DOI: 10.1016/j.jtice.2015.12.023

Guo, Y., Zhao, J., Zhang, H., Yang, S., Qi, J., Wang, Z., and Xu, H. (2005). "Use of rice husk-based porous carbon for adsorption of Rhodamine B from aqueous solutions," *Dyes Pigments* 66(2), 123-128. DOI: 10.1016/j.dyepig.2004.09.014

Gupta, V. K., Mohan, D., Sharma, S., and Sharma, M. (2000). "Removal of basic dyes (Rhodamine B and methylene blue) from aqueous solutions using bagasse fly ash," *Separ. Sci. Technol.* 35(13), 2097-2113. DOI: 10.1081/SS-100102091

Hu, L., Yuan, H., Zou, L., Chen, F., and Hu, X. (2015). "Adsorption and visible light-driven photocatalytic degradation of Rhodamine B in aqueous solutions by Ag@AgBr/SBA-15," *Appl. Surf. Sci.* 355, 706-715. DOI: 10.1016/j.apsusc.2015.04.166

Huo, S. H., and Yan, X. P. (2012). "Metal–organic framework mil-100(Fe) for the adsorption of malachite green from aqueous solution," *J. Mater. Chem. 22*(15), 7449-7455. DOI: 10.1039/C2JM16513A

Inyinbor, A. A., Adekola, F. A., and Olatunji, G. A. (2016). "Kinetics, isotherms and thermodynamic modeling of liquid phase adsorption of Rhodamine B dye onto *Raphia hookerie* fruit epicarp," *Water Resources and Industry* 15, 14-27. DOI: 10.1016/j.wri.2016.06.001

Khan, T. A., Sharma, S., and Ali, I. (2011). "Adsorption of Rhodamine B dye from aqueous solution onto acid activated mango (*Magnifera indica*) leaf powder: Equilibrium, kinetic and thermodynamic studies," *Journal of Toxicology and Environmental Health Sciences* 3(10), 286-297.

Kooh, M. R. R., Lim, L. B. L., Lim, L. H., and Dahri, M. K. (2016). "Separation of toxic Rhodamine B from aqueous solution using an efficient low-cost material, *Azolla pinnata*, by adsorption method," *Environ. Monit. Assess. 188*(2), 108. DOI: 10.1007/s10661-016-5108-7.

Liu, H., Ren, X., and Chen, L. (2016). "Synthesis and characterization of magnetic metal–organic framework for the adsorptive removal of Rhodamine B from aqueous solution," *J. Ind. Eng. Chem.* 34, 278-285. DOI: 10.1016/j.jiec.2015.11.020.

Luo, X., Liu, J., Wang, H., Huang, L., and Chen, L. (2014). "Comparison of hot-water extraction and steam treatment for production of high purity-grade dissolving pulp from green bamboo," *Cellulose* 21(3), 1445-1457. DOI: 10.1007/s10570-014-0234-2

Luo, X., and Zhu, J. Y. (2011). "Effects of drying-induced fiber hornification on enzymatic saccharification of lignocelluloses," *Enzyme. Microb. Tech.* 48(1), 92-99. DOI: 10.1016/j.enzmictec.2010.09.014

Nadupalli, S., Koorbanally, N., and Jonnalagadda, S. B. (2011). "Chlorine dioxide-facilitated oxidation of the azo dye amaranth," *J. Phys. Chem. A.* 115(42), 11682-11688. DOI: 10.1021/jp206175s

Obodai, M., Cleland-Okine, J., and Vowotor, K. A. (2003). "Comparative study on the growth and yield of *Pleurotus ostreatus* mushroom on different lignocellulosic by-products," *J. Ind. Microbiol. Biot.* 30(3), 146-149. DOI: 10.1007/s10295-002-0021-1

Panda, G. C., Das, S. K., and Guha, A. K. (2009). "Jute stick powder as a potential biomass for the removal of Congo red and Rhodamine B from their aqueous solution," *J. Hazard. Mater.* 164(1), 374-379. DOI: 10.1016/j.jhazmat.2008.08.015

Qu, L., Han, T., Luo, Z., Liu, C., Mei, Y., and Zhu, T. (2015). "One-step fabricated Fe_3O_4@C core–shell composites for dye removal: Kinetics, equilibrium and thermodynamics," *J. Phys. Chem. Solids* 78, 20-27. DOI: 10.1016/j.jpcs.2014.10.019

Ruthven, D. (1984). *Principles of Adsorption and Adsorption Processes*, John Wiley & Sons, New York, NY.

Shenvi, S. S., Isloor, A. M., Ismail, A. F., Shilton, S. J., and Al Ahmad, A. (2015). "Humic acid based biopolymeric membrane for effective removal of methylene blue and Rhodamine B," *Ind. Eng. Chem. Res.* 54(18), 4965-4975. DOI: 10.1021/acs.iecr.5b00761

Tan, D., Bai, B., Jiang, D., Shi, L., Cheng, S., Tao, D., and Ji, S. (2014). "Rhodamine B induces long nucleoplasmic bridges and other nuclear anomalies in *Allium cepa* root tip cells," *Environ. Sci. Pollut. R.* 21(5), 3363-3370. DOI: 10.1007/s11356-013-2282-9.

Tehrani, M. S., and Zare-Dorabei, R. (2016). "Highly efficient simultaneous ultrasonic-assisted adsorption of methylene blue and Rhodamine B onto metal organic framework MIL-68(Al): Central composite design optimization," *RSC Adv.* 6(33), 27416-27425. DOI: 10.1039/C5RA28052D

Tian, X., Li, C., Yang, H., Ye, Z., and Xu, H. (2011). "Spent mushroom: A new low-cost adsorbent for removal of congo red from aqueous solutions," *Desalin. Water Treat.* 27(1-3), 319-326. DOI: 10.5004/dwt.2011.2152

Toptas, A., Demierege, S., Ayan, E. M., and Yanik, J. (2014). "Spent mushroom compost as biosorbent for dye biosorption," *CLEAN - Soil Air Water* 42(12), 1721-1728. DOI: 10.1002/clen.201300657

Wang, S., Li, H., and Xu, L. (2006). "Application of zeolite MCM-22 for basic dye removal from wastewater," *J. Colloid. Interf. Sci.* 295(1), 71-78. DOI: 10.1016/j.jcis.2005.08.006

Wu, N., Wei, G., Lian, Y., Du, J., and Tie, X. (2017). "The transfer of natural Rhodamine B contamination from raw paprika fruit to capsicum oleoresin during the extraction process," *Food Chem.* 237, 786-792. DOI: 10.1016/j.foodchem.2017.05.147

Yan, T. G., and Wang, L. (2013). "Adsorptive removal of methylene blue from aqueous solution by spent mushroom substrate: Equilibrium, kinetics, and thermodynamics," *BioResources* 8(3), 4722-4734. DOI: 10.15376/biores.8.3.4722-4734

Zhang, L., Gao, H., and Liao, Y. (2016a). "Preparation and application of poly(AMPS-*co*-DVB) to remove Rhodamine B from aqueous solutions," *React. Funct. Polym.* 104, 53-61. DOI: 10.1016/j.reactfunctpolym.2016.05.001

Zhang, Y., Xie, C., Gu, F. L., Wu, H., and Guo, Q. (2016b). "Significant visible-light photocatalytic enhancement in Rhodamine B degradation of silver orthophosphate *via* the hybridization of N-doped graphene and poly(3-hexylthiophene)," *J. Hazard. Mater.* 315, 23-34. DOI: 10.1016/j.jhazmat.2016.04.068

Zhang, W., Shi, L., Tang, K., and Liu, Z. (2012). "Synthesis, surface group modification of 3D MnV_2O_6, nanostructures and adsorption effect on Rhodamine B," *Mater. Res. Bull.* 47(7), 1725–1733. DOI: 10.1016/j.materresbull.2012.03.038

Zhou, A., Zhang, Y., Li, R., Su, X., and Zhang, L. (2016). "Adsorptive removal of sulfa antibiotics from water using spent mushroom substrate, an agricultural waste," *Desalin. Water Treat.* 57(1), 388-397. DOI: 10.1080/19443994.2014.979239

Article submitted: July 19, 2017; Peer review completed: September 17, 2017; Revised version received and accepted: September 24, 2017; Published: September 29, 2017.
DOI: 10.15376/biores.12.4.8612-8628